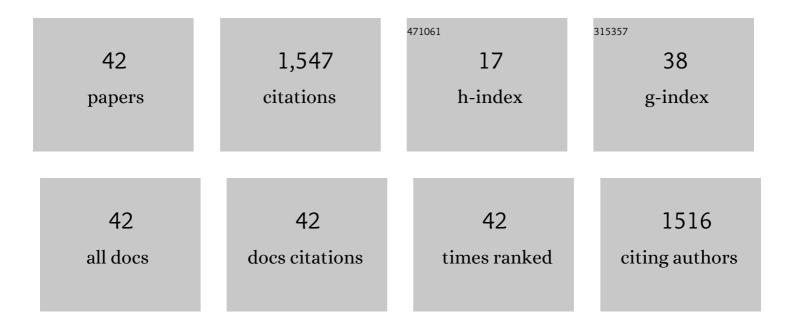
Qingming Huang

List of Publications by Year in descending order

Source: https://exaly.com/author-pdf/6820314/publications.pdf Version: 2024-02-01



#	Article	IF	CITATIONS
1	A novel double-perovskite Gd ₂ ZnTiO ₆ :Mn ⁴⁺ red phosphor for UV-based w-LEDs: structure and luminescence properties. Journal of Materials Chemistry C, 2016, 4, 2374-2381.	2.7	240
2	Synthesis and Characterization of Highly Efficient Near-Infrared Upconversion Sc ³⁺ /Er ³⁺ /Yb ³⁺ Tridoped NaYF ₄ . Journal of Physical Chemistry C, 2010, 114, 4719-4724.	1.5	144
3	Bandgap Tailoring via Si Doping in Inverse-Garnet Mg ₃ Y ₂ Ge ₃ O ₁₂ :Ce ³⁺ Persistent Phosphor Potentially Applicable in AC-LED. ACS Applied Materials & Interfaces, 2015, 7, 21835-21843.	4.0	143
4	Nonâ€Rareâ€Earth K ₂ XF ₇ :Mn ⁴⁺ (X = Ta, Nb): A Highlyâ€Efficient Narrowâ€Band Red Phosphor Enabling the Application in Wideâ€Colorâ€Gamut LCD. Laser and Photonics Reviews, 2017, 11, 1700148.	4.4	120
5	A highly-distorted octahedron with a C _{2v} group symmetry inducing an ultra-intense zero phonon line in Mn ⁴⁺ -activated oxyfluoride Na ₂ WO ₂ F ₄ . Journal of Materials Chemistry C, 2017, 5, 10524-10532.	2.7	120
6	Lu ₂ CaMg ₂ (Si _{1â^'x} Ge _x) ₃ O ₁₂ :Ce <s phosphors: bandgap engineering for blue-light activated afterglow applicable to AC-LED. Journal of Materials Chemistry C, 2016, 4, 10329-10338.</s 	sup>3+2.7	up>solid-solu 92
7	Resonance Emission Enhancement (REE) for Narrow Band Red-Emitting A ₂ GeF ₆ :Mn ⁴⁺ (A = Na, K, Rb, Cs) Phosphors Synthesized via a Precipitation–Cation Exchange Route. Inorganic Chemistry, 2017, 56, 11900-11910.	1.9	86
8	Structure and luminescence behavior of a single-ion activated single-phased Ba ₂ Y ₃ (SiO ₄) ₃ F:Eu white-light phosphor. Journal of Materials Chemistry C, 2017, 5, 1789-1797.	2.7	81
9	CsPbBr ₃ /EuPO ₄ dual-phase devitrified glass for highly sensitive self-calibrating optical thermometry. Journal of Materials Chemistry C, 2018, 6, 9964-9971.	2.7	68
10	A Photostimulated BaSi ₂ O ₅ :Eu ²⁺ ,Nd ³⁺ Phosphorâ€inâ€Glass for Erasableâ€Rewritable Optical Storage Medium. Laser and Photonics Reviews, 2019, 13, 1900006.	4.4	55
11	Synthesis of ZnO nanoparticle-anchored biochar composites for the selective removal of perrhenate, a surrogate for pertechnetate, from radioactive effluents. Journal of Hazardous Materials, 2020, 387, 121670.	6.5	55
12	Stress-induced CsPbBr3 nanocrystallization on glass surface: Unexpected mechanoluminescence and applications. Nano Research, 2019, 12, 1049-1054.	5.8	50
13	Low concentration Re(VII) recovery from acidic solution by Cu-biochar composite prepared from bamboo (Acidosasa longiligula) shoot shell. Minerals Engineering, 2018, 124, 123-136.	1.8	37
14	Improvement of photoluminescence properties and thermal stability of Y 2.9 Ce 0.1 Al 5 â^' x Si x O 12 phosphors with Si 3 N 4 addition. Journal of Alloys and Compounds, 2014, 615, 588-593.	2.8	33
15	Adsorption desulfurization performance and adsorption-diffusion study of B2O3 modified Ag-CeOx/TiO2-SiO2. Journal of Hazardous Materials, 2019, 362, 424-435.	6.5	33
16	Upcoversion performance improvement of NaYF4:Yb, Er by Sn codoping: Enhanced emission intensity and reduced decay time. Journal of Solid State Chemistry, 2013, 207, 170-177.	1.4	32
17	Upconversion Effective Enhancement by Producing Various Coordination Surroundings of Rare-Earth Ions. Inorganic Chemistry, 2015, 54, 2643-2651.	1.9	24
18	Fabrication of a stable poly(vinylpyrrolidone)/poly(urushiol) multilayer ultrathin film through layer-by-layer assembly and photo-induced polymerization. Colloids and Surfaces A: Physicochemical and Engineering Aspects, 2009, 337, 15-20.	2.3	15

QINGMING HUANG

#	Article	IF	CITATIONS
19	Synthesis of ERB-1 by a steam-environment crystallization method and further application in the post-synthesis of Ti-MWW zeolite. Applied Catalysis A: General, 2018, 564, 218-225.	2.2	13
20	Fast synthesis of hierarchical nanosized pure Si-Beta zeolite via a steam-assisted conversion method. Microporous and Mesoporous Materials, 2020, 293, 109675.	2.2	13
21	Tuning crystal field symmetry of hexagonal NaY0.92Yb0.05Er0.03F4 by Ti4+ codoping for high-performance upconversion. Journal of Alloys and Compounds, 2014, 613, 253-259.	2.8	12
22	The construction of Mo6â^'Î′O3â^'-supported catalyst for low-temperature propylene gas-phase epoxidation by Cu modification. Journal of Catalysis, 2018, 368, 120-133.	3.1	12
23	The surface construction of Mo–O–Bi coordination for high catalytic performance in gas-phase epoxidation of propylene with O ₂ . Catalysis Science and Technology, 2018, 8, 1070-1082.	2.1	10
24	Green synthesis of submicron-sized Ti-rich MWW zeolite powders via a novel mechanochemical dry gel conversion in mixed steam environment. Advanced Powder Technology, 2020, 31, 2025-2034.	2.0	10
25	Enhancement of photoluminescence properties and modification of crystal structures of Si3N4 doping Li2Sr0.995SiO4:0.005Eu2+ phosphors. Materials Research Bulletin, 2015, 70, 309-314.	2.7	9
26	Energy transfer between two luminescent centers and photoluminescent properties of Ca4-yLa6(AlO4) (SiO4)6-O1-/2: yEu2+apatite structure phosphors. Journal of Luminescence, 2021, 235, 117991.	1.5	9
27	Upconversion Performance Enhancement of NaYF ₄ :Yb/Tm by Codoping Hf ⁴⁺ as Energy Migrator. Acta Chimica Sinica, 2016, 74, 191.	0.5	5
28	Phosphorus modified MoO3–Bi2SiO5/SiO2 catalyst for gas-phase epoxidation of propylene by molecular oxygen. Research on Chemical Intermediates, 2017, 43, 7055-7071.	1.3	4
29	The construction of sublattice level energy cluster for promoting UV upconversion emission in tetragonal LiYF4. Journal of Alloys and Compounds, 2020, 821, 153544.	2.8	4
30	A General Synthesis Strategy for Highly Dispersed Amorphous MoO ₃ over Supported Catalysts. ChemistrySelect, 2016, 1, 2071-2078.	0.7	3
31	Structure and upconversion luminescence investigation of cubic Y3.2Yb0.4Er0.08Al0.32F12 codoped with Mg2+/Zn2+/Cu2+. Journal of Materials Science, 2017, 52, 4810-4819.	1.7	3
32	Rigid-resilient transition in calcium borosilicate sealing glass–ceramics: Effect of preferred orientation. Journal of the European Ceramic Society, 2018, 38, 2410-2416.	2.8	3
33	The Construction of Au–Fe–TS-1 Interface Coupling Structure for Improving Catalytic Performance of Propylene Epoxidation with H2 and O2. Catalysis Letters, 2020, 150, 3149-3158.	1.4	3
34	Synthesis of Different Morphology Er ³⁻ /Yb ³⁻ Codoped Hexagonal NaYF ₄ and Upconversion Luminescence Property Investigation. Acta Chimica Sinica, 2013, 71, 1071.	0.5	2
35	Sublattice Energy Cluster Construction for The Enhancement of NIR Photocatalytic Performance of LiYF ₄ : Tm@TiO ₂ . ChemistrySelect, 2019, 4, 4262-4270.	0.7	1
36	Phase Transition Induction and Upconversion Luminescence Enhancement of NaY _{0.95} ₋ <i>_x</i> Yb _{0.03} Er _{0.02} F ₄ b In ³ ⁺ Codoping. Acta Chimica Sinica, 2013, 71, 1639.	y0.5	1

QINGMING HUANG

#	Article	IF	CITATIONS
37	Study on the Upconversion Luminescence Mechanism of Tegtragonal LiYF4: RE with Sublattice Energy Cluster Construction and Crystal Field Manipulation. Acta Chimica Sinica, 2020, 78, 968.	0.5	1
38	Enhancement of Upconversion Luminescence by the Construction of a 3Yb-Er-Hf Sublattice Energy Cluster and Surface Defect Elimination. Inorganic Chemistry, 2022, 61, 5405-5412.	1.9	1
39	Preparation of Ni–Co–W–Si amorphous cosolute materials and study on adsorption properties. Materials Research Express, 2017, 4, 115204.	0.8	Ο
40	The constructing of Si-Fe-Sn co-solution surface of composite iron oxide catalyst via vapor methanol pretreatment and application in gaseous phenolic alkylation. Solid State Sciences, 2019, 87, 124-137.	1.5	0
41	Introduction of Biâ€Functional Cu/SiO 2 for Modulating the Chemical States of MoO 3 â€Bi 2 SiO 5 /SiO 2. ChemistrySelect, 2020, 5, 5771-5775.	0.7	Ο
42	Diatomite-Assisted Synthesis of Ordered Mesoporous Carbon and Its Application in Fuel Cells. Acta Chimica Sinica, 2012, 70, 1939.	0.5	0